

CONTENTS

1-11 Qifan Chen, Xiaofeng Liu, Zhihao Guo, Xiaoxu Xu & Yanhua Lu (2018) Synthesis and characterization of new chiral liquid crystal monomers containing steroid unit, *Molecular Crystals and Liquid Crystals*, 669:1, 1-11, DOI: [10.1080/15421406.2018.1553744](https://doi.org/10.1080/15421406.2018.1553744)

ISSN: 1542-1406 (Print) 1563-5287 (Online) Journal homepage: <https://www.tandfonline.com/loi/gmcl20>

Synthesis and characterization of new chiral liquid crystal monomers containing steroid unit

Qifan Chen, Xiaofeng Liu, Zhihao Guo, Xiaoxu Xu & Yanhua Lu

To cite this article: Qifan Chen, Xiaofeng Liu, Zhihao Guo, Xiaoxu Xu & Yanhua Lu (2018) Synthesis and characterization of new chiral liquid crystal monomers containing steroid unit, *Molecular Crystals and Liquid Crystals*, 669:1, 1-11, DOI: [10.1080/15421406.2018.1553744](https://doi.org/10.1080/15421406.2018.1553744)

To link to this article: <https://doi.org/10.1080/15421406.2018.1553744>



Published online: 07 May 2019.



Submit your article to this journal [↗](#)



View Crossmark data [↗](#)



Synthesis and characterization of new chiral liquid crystal monomers containing steroid unit

Qifan Chen^a, Xiaofeng Liu^b, Zhihao Guo^b, Xiaoxu Xu^a, and Yanhua Lu^{a,c}

^aSchool of Chemical Engineering, Eastern Liaoning University, Dandong, P. R. China; ^bCenter for Molecular Science and Engineering, College of Science, Northeastern University, Shenyang, P. R. China;

^cKey Laboratory of Functional Textile Materials, Liaoning Province, Dandong, P. R. China

ABSTRACT

To reduce the bulky steric hindrance, improve the reactivity of diosgenin and cholesterol, and obtain mesophase of their derivatives, the commercially available cholesterol and diosgenin were allowed to be structurally modified. Four new chiral LC intermediate compounds (**c**–**f**) and the corresponding monomers (**M**₁–**M**₄) with different longer spacer were synthesized. The chemical structures, optical texture, thermal behavior and mesophase structure of all the mesogenic compounds obtained in this study were characterized by FT-IR, ¹H-NMR, polarizing optical microscopy, differential scanning calorimetry, and X-ray diffraction measurements. The experimental results showed that the intermediate compounds containing diosgenyl groups **c** and **d** only showed a mesophase and exhibited fan-shaped texture of a smectic A (*S*_A) phase, while the compounds containing terminal cholesteryl groups **e** and **f** showed two mesophases and exhibited fan-shaped texture of a *S*_A phase, and oily streak texture and focal conic texture of cholesteric phase, respectively. The four chiral monomers **M**₁–**M**₄ all revealed cholesteric oily streak texture and focal conic texture. In addition, the melting temperature (*T*_m) and isotropic temperature (*T*_i) of the mesogenic compounds decreased with increasing the flexible spacer length. Compared with the intermediate compounds or monomers based on cholesterol, the compounds or monomers based on diosgenin showed higher *T*_m and *T*_i.

KEYWORDS

diosgenin; cholesterol;
liquid crystal;
monomer; chiral

1. Introduction

Liquid crystal (LC) materials have been widely used for display devices because their flexible ordered structures can lead to systems displaying switchable optical modulation. The LC compounds can potentially be used as new functional materials for electron, ion, molecular transporting, sensory, catalytic, optical and bioactive materials [1, 2]. In recent year, chiral LC compounds with helical supramolecular structure are always fascinating and have attracted considerable attention and interest because they possess excellent electro-optical properties, including selective reflection of light, thermochromism, ferroelectricity, and circular dichroism, and important potential applications in various areas such as non-linear optical devices, flat-panel displays, thermal imaging, rewritable

full-color image recording, and photostable UV screens [3–17]. Chirality can be introduced into LC molecules at various levels, and be divided into three types, including point chirality, axial chirality (e.g. BINOL) [18, 19] and planar chirality (e.g. phanes) [20]. Point chirality is usually introduced as a branching point somewhere in the alkyl-tail of a liquid crystal, but some are located in the terminal position of the mesogenic core, such as steroids. The cholesteric phase is formed by rod-like, chiral molecules responsible for macroscopical alignment of cholesteric domains. Depending to chemical structures, it may be feasible to achieve a macroscopic alignment of cholesteric domains. In general, the formation of mesophases may be affected by aspect ratio, flexible spacer at the center, and polarity of the monomers [21, 22].

As a kind of natural mesogen, diosgenin and cholesterol with many chiral centers have a strong optical activity or high specific optical rotation [23]. Until now, they have become an attractive candidate to synthesize new LC materials [24–30]. Therefore, it would be both necessary and useful to synthesize various kinds of chiral LC materials to explore their potential applications. In the present work, we aimed to design new chiral LC materials based on diosgenin and cholesterol. To investigate the effect of spacer length and terminal groups on molecular interaction and physical properties of the chiral materials, four new chiral LC intermediate compounds and the monomers with different longer spacer were synthesized. Their structure and phase behavior were characterized using FTIR, ^1H NMR, POM, DSC, and XRD.

2. Experimental method

2.1. Materials

All chemicals were obtained from the indicated sources. Tosyl chloride, methacrylic acid, palladium 10% on carbon and benzyl chloride were purchased from Sinopharm Chemical Reagent Co., Ltd. (Shenyang, China). 1,6-Hexanediol and 1,8-octanediol were purchased from Qingdao Lilai Fine Chemical Industry Co., Ltd. (Qingdao, China). Diosgenin was purchased from Wuhan Chemical Industry Co., Ltd. (Wuhan, China). Cholesterol was purchased from Xiayi Beier Biological Products Co., Ltd. (Xiayi, China). All other solvents and reagents used were purified by standard methods.

2.2. Measurements

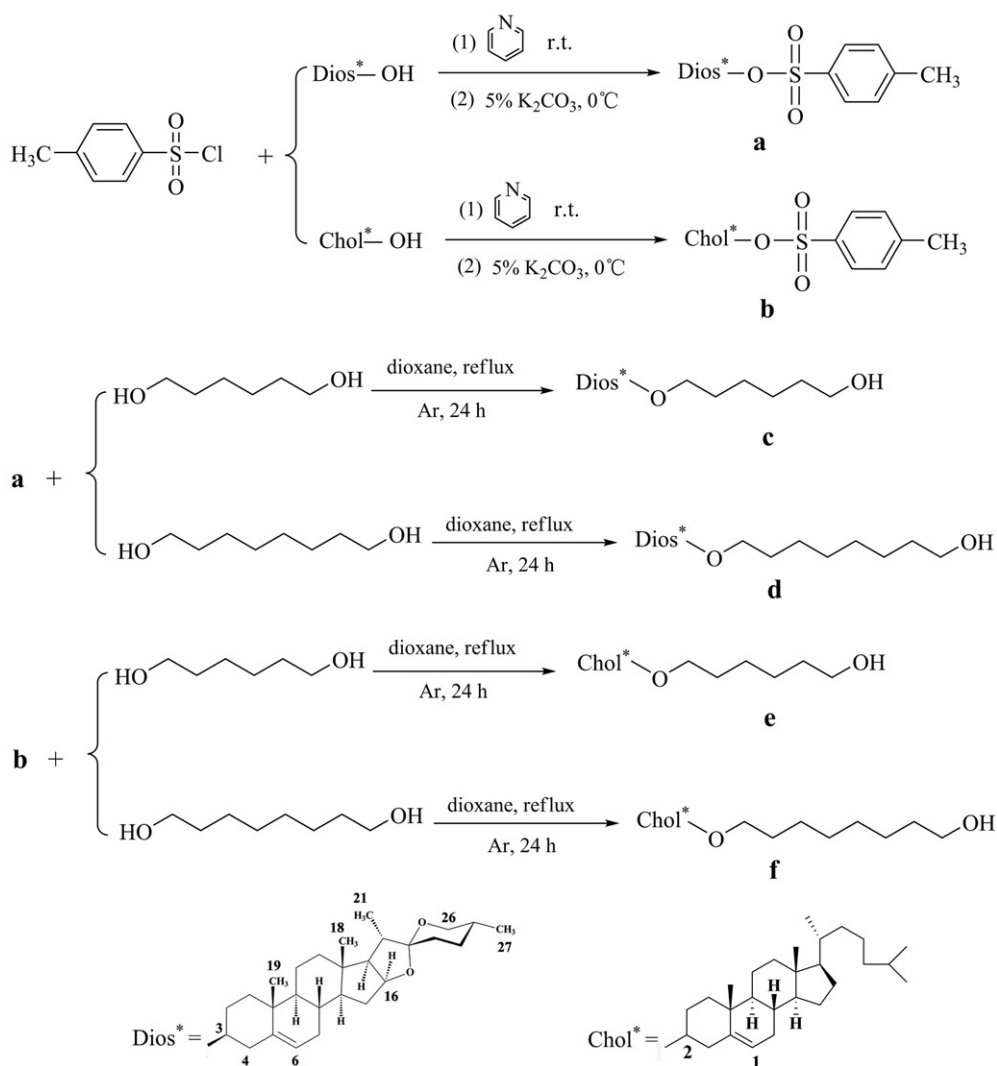
FTIR spectra were measured on a PerkinElmer spectrum One (B) spectrometer (PerkinElmer, Foster City, CA). ^1H NMR spectra were obtained using a Bruker ARX 600 (Bruker, Fällanden, Swiss) high resolution NMR spectrometer, and chemical shifts were reported in ppm with tetramethylsilane (TMS) as an internal standard. The optical texture was observed with a Leica DMRX POM (Leica, Wetzlar, Germany) equipped with a Linkam THMSE-600 (Linkam, London, UK) cool and hot stage. The thermal behavior was determined with a Netzsch DSC 204 (Netzsch, Hanau, Germany) equipped with a cooling system. XRD measurements were performed with a nickel-filtered Cu-K_α radiation with a Bruker D8 Advance (Bruker, Germany) powder diffractometer.

2.3. Synthesis of the intermediate compounds

The synthetic route of the intermediate compounds **a-f** is outlined in Scheme 1. Diosgenyl-*p*-toluene sulfonate (**a**), cholesteryl-*p*-toluene sulfonate (**b**), 6-diosgenoxyhexane-1-ol (**c**), 8-diosgenoxyoctane-1-ol (**d**), 6-cholesteroxyhexane-1-ol (**e**) and 8-cholesteroxyoctane-1-ol (**f**) were synthesized as described in the literatures [31–34].

2.3.1. Synthesis of 6-diosgenoxyhexane-1-ol (**c**)

Yield: 73%, mp: 109.8 °C. IR (KBr, cm^{-1}): 3333 (–OH); 2929, 2850 (CH_3 –, $-\text{CH}_2$ –); 1241, 1097 (C–O–C). ^1H NMR (δ , CDCl_3 , 600 MHz): 5.34 (t, 1H, **H-6**), 4.41(q, 1H, **H-**



Scheme 1. Synthetic route of the compounds a–f.

16), 3.64 (t, 2H, HOCH₂-), 3.49-3.38 (m, 4H, **H**-26 and HOCH₂CH₂O-), 3.12 (m, 1H, **H**-3), 2.37-0.80 [m, 44H, **H**-diosgenyl and -(CH₂)₄-].

2.3.2. Synthesis of 8-diosgenoxyhexane-1-ol (d)

Yield: 65%, mp: 105.2 °C. IR (KBr, cm⁻¹): 3372 (-OH); 2930, 2855 (CH₃-, -CH₂-); 1242, 1080 (C-O-C). ¹H NMR (δ, CDCl₃, 600 MHz): 5.34 (t, 1H, **H**-6), 4.41(q, 1H, **H**-16), 3.64 (t, 2H, HOCH₂-), 3.48-3.43 (m, 4H, **H**-26 and HOCH₂CH₂O-), 3.12 (m, 1H, **H**-3), 2.37-0.80 [m, 48H, **H**-diosgenyl and -(CH₂)₆-].

2.3.3. Synthesis of 6-cholesteroxyhexane-1-ol (e)

Yield: 64%, mp: 66.2 °C. IR (KBr, cm⁻¹): 3339 (-OH); 2934, 2851 (CH₃-, -CH₂-); 1241, 1097 (C-O-C). ¹H NMR (δ, CDCl₃, 600 MHz): 5.38 (t, 1H, **H**-1), 3.65 (t, 2H, HOCH₂-), 3.42 (m, 2H, HOCH₂CH₂O-), 3.10 (m, 1H, **H**-2), 2.33-0.68 [m, 51H, **H**-cholesteryl and -(CH₂)₄-].

2.3.4. Synthesis of 8-cholesteroxyoctan-1-ol (f)

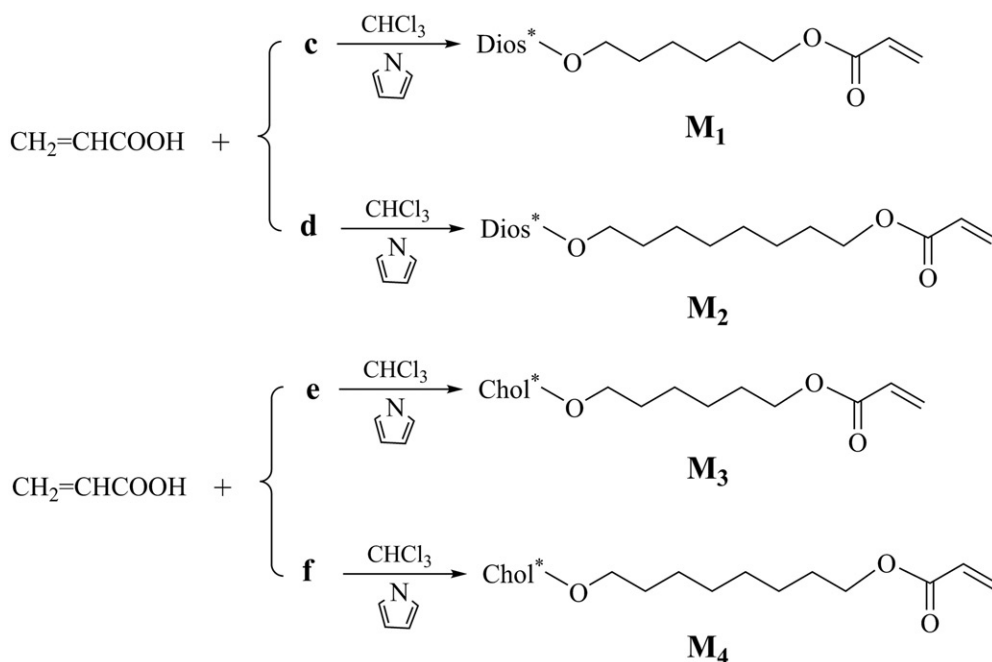
Yield: 62%, mp: 66.0 °C. IR (KBr, cm⁻¹): 3394 (-OH); 2933, 2852 (CH₃-, -CH₂-); 1266, 1057 (C-O-C). ¹H NMR (δ, CDCl₃, 600 MHz): 5.37 (t, 1H, **H**-1), 3.65 (t, 2H, HOCH₂-), 3.43 (m, 2H, -CH₂CH₂O-), 3.12 (m, 1H, **H**-2), 2.34-0.68 [m, 55H, **H**-cholesteryl and -(CH₂)₆-].

2.4. Synthesis of chiral monomers

The synthetic route of the chiral monomers **M**₁-**M**₄ is outlined in Scheme 2. They were synthesized using the same method, and the detailed synthetic process of **M**₁ is described as follows as an example.

2.4.1. Synthesis of 6-diosgenoxyhexyl acrylate (**M**₁)

The compound **c** (2.06 g, 3 mmol), dried chloroform (15 mL), pyridine (5 mL) and a small amount of hydroquinone were placed in a three-neck flask with a magnetic stir bar and then acryloyl chloride was added dropwise. The system was reacted for 2 h at room temperature and for 5 h at 45 °C. After that, the mixture was cooled to temperature and poured into methyl alcohol, and there were white precipitates appeared. The crude product was purified by silica gel column chromatography (ethyl acetate/hexane =1:1) to result in white solid. Yield: 47%. IR (KBr, cm⁻¹): 2932, 2852 (CH₃-, -CH₂-); 1730 (C=O); 1641 (C=C); 1231 (C-O-C). ¹H NMR (δ, CDCl₃, 600 MHz): 6.38 (m, 1H, CH₂=, *trans*-), 6.11 (m, 1H, =CH-), 5.75 (m, 1H, CH₂=, *cis*-), 5.34 (t, 1H, **H**-6), 4.42(q, 1H, **H**-16), 3.64 (t, 2H, HOCH₂-), 3.49-3.37 (m, 4H, **H**-26 and -CH₂CH₂O-), 3.12 (m, 1H, **H**-3), 2.37-0.79 [m, 44H, **H**-diosgenyl and -(CH₂)₄-].



Scheme 2. Synthetic route of the monomers M1–M4.

2.4.2. Synthesis of 8-diosgenyloxyoctyl acrylate (M_2)

In a way similar to the synthesis of M_1 , new diosgenyl derivative M_2 was accordingly prepared. Yield: 42%. IR (KBr, cm^{-1}): 2932, 2855 (CH_3 -, $-\text{CH}_2$ -); 1735 ($\text{C}=\text{O}$); 1643 ($\text{C}=\text{C}$); 1238, ($\text{C}-\text{O}-\text{C}$). ^1H NMR (δ , CDCl_3 , 600 MHz): 6.37 (m, 1H, $\text{CH}_2=$, *trans*-), 6.10 (m, 1H, $=\text{CH}$ -), 5.77 (m, 1H, $\text{CH}_2=$, *cis*-), 5.33 (t, 1H, **H**-6), 4.41(q, 1H, **H**-16), 3.64 (t, 2H, HOCH_2 -), 3.48-3.42 (m, 4H, **H**-26 and $\text{HOCH}_2\text{CH}_2\text{O}$ -), 3.13 (m, 1H, **H**-3), 2.37-0.79 [m, 48H, **H**-diosgenyl and $-(\text{CH}_2)_6$ -].

2.4.3. Synthesis of 6-cholesteryloxyhexyl acrylate (M_3)

In a way similar to the synthesis of M_1 , new cholesteryl derivative M_3 was accordingly prepared. Yield: 64%. IR (KBr, cm^{-1}): 2935, 2850 (CH_3 -, $-\text{CH}_2$ -); 1730 ($\text{C}=\text{O}$); 1642 ($\text{C}=\text{C}$); 1240 ($\text{C}-\text{O}-\text{C}$). ^1H NMR (δ , CDCl_3 , 600 MHz): 6.35 (m, 1H, $\text{CH}_2=$, *trans*-), 6.12 (m, 1H, $=\text{CH}$ -), 5.76 (m, 1H, $\text{CH}_2=$, *cis*-), 5.38 (t, 1H, **H**-1), 3.65 (t, 2H, HOCH_2 -), 3.41 (m, 2H, $\text{HOCH}_2\text{CH}_2\text{O}$ -), 3.12 (m, 1H, **H**-2), 2.33-0.68 [m, 51H, **H**-cholesteryl and $-(\text{CH}_2)_4$ -].

2.4.4. Synthesis of 8-cholesteryloxyoctyl acrylate (M_4)

In a way similar to the synthesis of M_1 , new cholesteryl derivative M_4 was accordingly prepared. Yield: 43%. IR (KBr, cm^{-1}): 2934, 2851 (CH_3 -, $-\text{CH}_2$ -); 1732 ($\text{C}=\text{O}$); 1641

(C=C); 1262 (C–O–C). ^1H NMR (δ , CDCl_3 , 600 MHz): 6.36 (m, 1H, $\text{CH}_2=$, *trans*-), 6.13(m, 1H, =CH-), 5.76 (m, 1H, $\text{CH}_2=$, *cis*-), 5.37 (t, 1H, **H**-1), 3.64 (t, 2H, HOCH_2-), 3.43 (m, 2H, $\text{HOCH}_2\text{CH}_2\text{O}-$), 3.12 (m, 1H, **H**-2), 2.33-0.69 [m, 51H, **H**-cholesteryl and $-(\text{CH}_2)_4-$].

3. Results and discussion

3.1. Optical textures

POM was used to observe the optical textures of liquid crystal (LC) intermediates and monomers. POM can not only clearly observe the typical textures of the mesophase, but also record the melting temperature (T_m), the LC phase transition temperature, and the isotropic temperature (T_i).

3.1.1. Optical textures of the intermediates

As the POM results, the intermediate **c** exhibited the fan-shaped texture of a smectic A (S_A) phase at 118 °C, and heated to 135.0 °C, the texture disappeared. When cooled to 131.0 °C, the fan-shaped texture of a S_A phase started to appear and grew up with the decrease of temperature. Continued cooling to 40 °C, crystallization phenomenon appeared. The intermediate **d** started to melt at 101 °C, and exhibited the fan-shaped texture of a S_A phase at 111 °C, and an isotropic phase was observed at 121 °C. On the cooling process, the fan-shaped texture of a S_A phase appeared at 115 °C, and crystallized at 64 °C. The intermediate **e** started to melt at 64 °C, and showed the fan-shaped texture of a S_A phase at 81 °C and oily streak texture of cholesteric phase at 91 °C. The texture disappeared 98 °C. When cooled to 93 °C, the focal conic texture appeared, and no crystallization phenomenon was observed during the cooling process. The intermediate **f** melted at 64 °C, and exhibited the fan-shaped texture of a S_A phase at 70 °C and oily streak texture of cholesteric phase at 73 °C. Continued heating, the texture disappeared at 87 °C. When cooled to 80 °C, the focal conic texture appeared. As an example, the optical textures of the compound **f** at different temperatures are shown in Figure 1.

In general, the mesomorphic properties of LC compounds depend on the terminal groups, the rigidity of the LC core and the flexible spacer length. For the intermediates

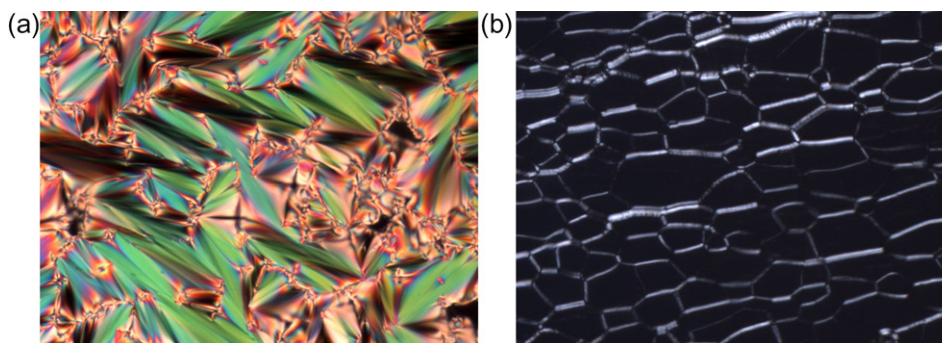


Figure 1. Optical textures of the compound **f** (200 \times) (a) fan-shaped texture of a S_A phase on heating to 70 °C, (b) oily streak texture of cholesteric phase on heating to 73 °C.

c-f, the chiral terminal groups exhibited obvious effect on the phase behavior. For example, the intermediates **c** and **d** with diosgenin groups only showed smectic phase, however, the intermediates **e** and **f** with cholesteryl groups showed both smectic phase and cholesteric phase.

3.1.2. Optical textures of the monomers

The monomers M_1 - M_4 showed enantiotropic mesophase with the oily streak texture and the focal conic texture of cholesteric phase during heating and cooling cycles, which was also confirmed by XRD analysis. Herein, M_4 was chosen as a representative to discuss the mesophase behavior in detail. On the heating process, M_4 showed oily streak texture of cholesteric phase at 55 °C, along with selective reflection phenomenon, and the reflection shifted to blue wavelength with the increase of the temperature. When heated to 112 °C, the texture disappeared. On the cooling process, the typical focal conic texture appeared at 108 °C and grew up with the decrease of the temperature. If a shear force was applied to the sample at the moment, the focal conic texture immediately changed to the oil streak texture, which was the characteristic of cholesteric phase. The optical textures of the monomer M_4 are shown in Figure 2.

3.2. Thermal behaviors

DSC was used to study the thermal behavior of the LC intermediates and monomers. The corresponding phase transition temperatures and enthalpy changes were obtained during first cooling and second heating scans.

3.2.1. Thermal behavior of the intermediates

The thermal analytical results of the intermediates **c-f** are summarized in Table 1. According to DSC curves, the intermediates **c** and **d** only showed an endothermic peak on heating process and an exothermic peak on cooling process, which represented the melting temperature and crystallization transition temperature. There was no transition peak between the mesophase and isotropic state. However, the fan-shaped texture of a

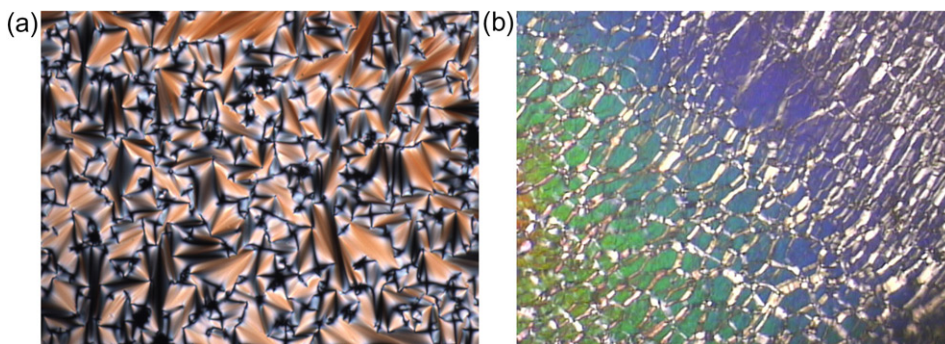


Figure 2. Optical textures of the monomer M_4 (200 \times) (a) focal conic texture of cholesteric phase on cooling to 108 °C, (b) oily streak texture of cholesteric phase on heating to 55 °C.

Table 1. Thermal properties of intermediate compounds **c**~**f**.

Compound	Phase transition temperature (°C) and enthalpy changes (J·g ⁻¹)	
	heating cycle	cooling cycle
c	K109.8(30.1) S _A 135.2 ^a (-)	1128.2(7.1)S _A -K
d	K105.2(28.8) S _A 121.3 ^a (-)	1107.9(6.0)S _A -K
e	K66.4(24.2)S _A 90.9(1.3)Ch98.8(1.1)	197.8(1.2)Ch89.6(1.2)S _A 21.9(46.9)K
f	K66.2(23.3)S _A 75.9(0.5)Ch87.2(1.1)	186.3(1.3)Ch68.2(0.4)S _A 13.8(6.8)K

K = crystal; S_A = smectic A phase; Ch = cholesteric phase; | = isotropic. ^aData obtained with POM

smectic phase was observed by the POM. For example, the melting range of the intermediate **c** was from 119 to 139 °C on the DSC results, and according to the POM result, the intermediate **c** exhibited isotropic phase transition at 135 °C and the isotropic temperature range was quite narrow.

The intermediates **e** and **f** showed three endothermic peaks on heating process and three exothermic peaks on cooling process. On heating curves, the peak at low temperature represented the melting phase transition, the second peak represented a S_A phase to cholesteric phase transition, and the peak at high temperature represented cholesteric phase to isotropic phase transition. Three exothermic peaks on the cooling curves represented an isotropic to cholesteric phase transition, a cholesteric to S_A phase transition and crystallization transition, respectively.

The terminal groups, the rigidity of the LC core and the flexible spacer length have an obvious effect on the thermal behavior of LC compounds. As seen from the data in Table 1, compared with the intermediates with terminal diosgenyl groups, those with terminal cholesteryl groups had a lower melting temperature (T_m), lower isotropic temperature (T_i) and wider mesophase temperature range (ΔT). For example, the T_m , T_i and ΔT of the intermediate **e** were 66.4 °C, 98.8 °C and 32.4 °C, while the T_m of the compound **c** was 109.8 °C, and the T_i and ΔT obtained from POM were 135.2 °C and 25.4 °C, respectively. Furthermore, a longer spacer could cause the decrease of the T_m , T_i , and ΔT . For example, compared with the intermediate **e** with six methylene spacer, the T_m , T_i and ΔT of the intermediate **f** with eight methylene spacer decreased by 0.2 °C, 11.6 °C and 12.4 °C, respectively.

3.2.2. Thermal behavior of the monomers

The phase transition temperature of the monomers **M**₁-**M**₄ is summarized in Table 2. As the DSC curves, the monomers **M**₁ and **M**₂ with diosgenyl groups showed a glass transition and a cholesteric to isotropic phase transition, which indicated they were amorphous LC compounds. However, the monomers **M**₃ and **M**₄ with cholesteryl groups showed the melting transition and a cholesteric to isotropic phase transition, which indicated they were crystalline LC compounds. All of these indicated that the terminal groups and the flexible spacer length had a similar effect on the thermal behavior of monomers similar to intermediates.

Table 2. Thermal properties of monomers M_1 – M_4 .

Monomer	Phase transition temperature ($^{\circ}\text{C}$) and enthalpy changes ($\text{J}\cdot\text{g}^{-1}$)	
	heating cycle	cooling cycle
M_1	G21.6Ch111.9(1.7)I	I101.9(1.8)Ch–G
M_2	G11.6Ch113.0(5.6)I	I110.8(4.1)Ch–G
M_3	K98.7(31.8)Ch109.7(0.9)I	I108.3(1.0)Ch67.3(23.0)K
M_4	K40.5(7.8)Ch57.8(0.8)I	I55.3(1.2)Ch40.4(–)K

G = glass; K = crystal; Ch = cholesteric phase; I = isotropic.

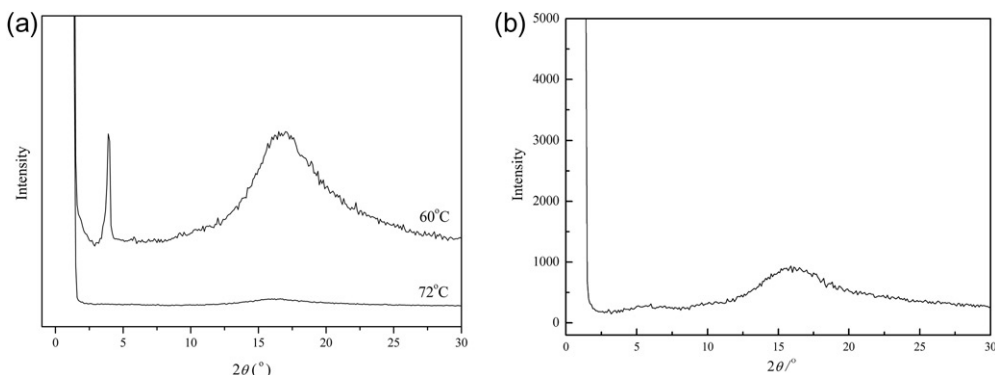


Figure 3. XRD patterns of (a) the intermediate **f** at 60 and 72 $^{\circ}\text{C}$, and (b) the monomer M_4 at 50 $^{\circ}\text{C}$.

3.3. Mesophase structure

XRD measurement was used to further study the mesophase structure of the LC compounds, especially the determination of the smectic phase and the study of the molecular orientation. In general, there is a Bragg scattering ($1^{\circ} < 2\theta < 5^{\circ}$) for the smectic phase, and no peak in the small-angle region for the nematic or cholesteric phase.

The XRD measurement of the intermediates and monomers in variable temperature attached to different mesophase range was carried out. The XRD patterns of the intermediates **c** and **d** showed a sharp reflection at small-angle region. For **e** and **f**, their XRD patterns at low temperature revealed a sharp reflection at small-angle region, but those at high temperature only showed a broad peak at wide-angle region. Combined with the POM results, the intermediates **c** and **d** could be confirmed as a S_A phase, and **e** and **f** showed a S_A phase at low temperature and a cholesteric phase at high temperature. For example, the compound **f** at low temperature revealed a strong peak at $2\theta = 3.92^{\circ}$, which represented that the molecules arranged in layers with short range, and the corresponding d -spacing was estimated to be 22.5 Å, however the compound **f** at high temperature displayed a broad peak at $2\theta = 16.9^{\circ}$. Furthermore, the XRD patterns of the monomers M_1 – M_4 only showed a broad peak at wide-angle region, which were confirmed to be a cholesteric phase according to the oily streak texture and the focal conic texture observed with POM. As an example, the XRD curves of the intermediate **f** at 60 and 72 $^{\circ}\text{C}$, and the monomer M_4 at 50 $^{\circ}\text{C}$ are shown in Figure 3.

4. Conclusions

In this work, we reported four LC intermediates and their corresponding acrylate monomers with diosgenyl or cholesteryl groups. The intermediates **c** and **d** exhibited a S_A phase, and **e** and **f** showed a S_A phase and cholesteric phase, while four monomers **M₁-M₄** only showed a cholesteric phase. Compared with the compounds with terminal diosgenin groups, that with terminal cholesteryl groups had a lower T_m , lower T_i and broader mesophase temperature range. Furthermore, a longer spacer could cause the decrease of the T_m and T_i and the narrowing of the mesophase temperature range.

Acknowledgements

This work was supported by the National Natural Science Foundation of China (51873084), Department of Education of Liaoning Province (ldxy2017002), and Science and Technology Committee of Liaoning Province (201602342).

References

- [1] Kato, T.; Mizoshita, M.; Kishimoto, K. (2006) *Angew. Chem. Int. Ed.*, 45, 38.
- [2] Bisoyi, H. K.; Humar, S. (2011) *Chem. Soc. Rev.*, 40, 306.
- [3] Takeda, M.; Kitazume, T.; Yamazaki, T.; Koden, M. (1995) *J. Mater. Sci.*, 30, 5199.
- [4] Palfy-Muhoray, P. (1998) *Nature* 391, 745.
- [5] Kim, Y. B.; Hur, I. K.; Choi, J. W.; Buivydas, M.; Gouda, F.; Lagerwall, S. T. (2000) *J. Mater. Sci.*, 35, 5457.
- [6] Watanabe, J.; Kamee, H.; Fujiki, M. (2001) *Polym. J.*, 33, 495.
- [7] Percec, V.; Obata, M.; Rudick, J. G.; De, B. B.; Glodde, M. (2002) *J. Polym. Sci. Part A: Polym. Chem.*, 40, 3509.
- [8] Shibaev, P. V.; Kopp, V. I.; Genack, A. Z. (2003) *J. Phys. Chem., B* 107, 6961.
- [9] Hu, J. S.; Zhang, B. Y.; Pan, W.; Zhou, A. J. (2005) *Liq. Cryst.*, 32, 441.
- [10] Brettar, J.; Burgi, T.; Donnio, B.; Guillon, D.; Klappert, R.; Scharf, T.; Deschenaux, R. (2006) *Adv. Funct. Mater.*, 16, 260.
- [11] Ohta, R.; Togashi, F.; Goto, H. (2007) *Macromolecules* 40, 5228.
- [12] Gupta, V. K.; Sharma, R. K.; Mathews, M.; Yelamaggad, C. V. (2009) *Liq. Cryst.*, 36, 339.
- [13] Hu, J. S.; Li, D.; Zhang, W. C.; Meng, Q. B. (2012) *J Polym Sci Part A: Polym Chem.*, 50, 5049.
- [14] Wang, Y.; Li, Q. (2012) *Adv. Mater.*, 24, 1926.
- [15] Uchida, Y.; Takanishi, Y.; Yamamoto, J. (2013) *Adv. Mater.*, 25, 3234.
- [16] Bruckner, J. R.; Porada, J. H.; Dietrich, C. F.; Dierking, I.; Giesselmann, F. (2013) *Angew Chem. Int. Ed.*, 52, 8934.
- [17] Liu, Y.; Xu, X. X.; Su, D.; Guo, Z. H.; Chen, Q. F.; Hu, J. S. (2017) *Mol. Cryst. Liq. Cryst.*, 658, 108.
- [18] Eelkema, R.; Feringa, B. L. (2007) *Org. Biomol. Chem.*, 38, 3729.
- [19] Kuball, H. G.; Bernhard, W.; Beck, A. K.; Seebach, D. (1997) *Helv. Chim. Acta* 80, 2507.
- [20] Mandle, R. J.; Goodby, J. W. (2018) *Liq. Cryst.*, 45, 1567.
- [21] Collings, P. J.; Hird, M. (1997) *Introduction to Liquid Crystals Chemistry and Physics*; Taylor & Francis: London, Chapter 3.
- [22] Liu, J. H.; Hung, H. J.; Yang, P. C.; Tien, K. H. (2008) *J. Polym. Sci. Part A: Polym. Chem.*, 46, 6214.
- [23] Mitov, M. (2012) *Adv. Mater.*, 24, 6260.
- [24] Wang, B.; Du, H. Y.; Zhang, J. H. (2011) *Steroids* 76, 204.
- [25] Dierking, I.; Kosbar, L. L.; Held, G. A. (1998) *Liq. Cryst.*, 24, 387.

- [26] Jia, L.; Cao, A.; Lévy, D.; Xu, B.; Albouy, P. A.; Xing, X. J.; Bowic, M. J.; Li, M. H. (2009) *Soft Matter*, 5, 3446.
- [27] Jia, L.; Lévy, D.; Durand, D.; Impéror-Clerc, M.; Cao, A.; Li, M. H. (2011) *Soft Matter*, 7, 7395.
- [28] Guo, Z. H.; Liu, X. F.; Hu, J. S.; Yang, L. Q.; Chen, Z. P. (2017) *Nanomaterials*, 7, 169
- [29] Xu, X. X.; Liu, X. F.; Li, Q.; Hu, J. S.; Chen, Q. F.; Yang, L. Q.; Lu, Y. H. (2017) *RSC Adv.*, 7, 14176.
- [30] Xie, Y. J.; Liu, X. F.; Hu, Z.; Hou, Z. P.; Guo, Z. H.; Chen, Z. P.; Hu, J. S.; Yang, L. Q. (2018) *Nanomaterials*, 8, 195.
- [31] Yao, D, S., Li, P., Liu, X. F., Hu, J. S., & Yang, L. Q. (2015). *Colloid Polym. Sci.*, 293, 3049.
- [32] Yang, J., Li, Q., Li, Y. (2006). *J. Polym. Sci. Part A: Polym. Chem.*, 44, 2045.
- [33] Guo, Z. H., Li, P., Liu, X. F., Yang, L. Q., Hu, J. S., & Chen, Z. P. (2018). *Liq. Cryst.*, 45, 886.
- [34] Liu, X. F., Guo, Z. H., Xie, Y. J., Chen, Z. P., Hu, J. S., & Yang, L. Q. (2018). *J. Mol. Liq.*, 259, 350.